Analysis and comparison of multiple-delay schemes for controlling unstable fixed points of discrete maps

Joshua E. S. Socolar and Daniel J. Gauthier
Physics Department and Center for Nonlinear and Complex Systems, Duke University, Durham, North Carolina 27708
(Received 20 January 1998)

We investigate theoretically the stabilization of a fixed point of a discrete one-dimensional nonlinear map by applying small perturbations to an accessible system parameter or variable. The size of the perturbations is determined in real time using feedback schemes incorporating only the dynamical state of the system and its state at previous iterates without making a comparison to a reference state. In particular, we compare and contrast two algorithms: extended time-delay autosynchronization, which uses an infinite series of past iterates with weights that decay by a factor of R with each time step, and N-time-delay autosynchronization, which uses an average of N past iterates with equal weights. The range of feedback parameters that successfully stabilize the fixed point and the robustness of the schemes to noise are determined. It is found that the domain of control for the two schemes is similar for appropriately matched values of R and N, and that N-time-delay autosynchronization tends to be less sensitive to noise.
[S1063-651X(98)02706-8]

PACS number(s): 05.45.+b, 07.05.Dz, 87.22.−q

I. INTRODUCTION

It is now well established that instabilities and chaos occurring in nonlinear dynamical systems can be controlled effectively by applying only small perturbations to an accessible system parameter or variable [1]. The most common class of control techniques relies on feedback of an error signal proportional to the difference between the current state of the system and a known reference state [2,3]. For systems in which production of the reference signal is impossible, either due to the high frequencies involved or the spatial complexity of the desired behavior, time-delay feedback is a natural option to explore [4–17]. In time-delay feedback schemes, the past behavior of the system is substituted for the predetermined reference state, so that the system itself provides a useful error signal. With the delay time chosen to be equal to the period of the desired orbit, the difference between past and current states vanishes when the system is on that orbit, so that the controlled behavior remains a solution to the original system's equations of motion and only small perturbations are applied. It has been argued elsewhere that time-delay approaches are appropriate, or perhaps necessary, in applications ranging from diode laser stabilization [10] to suppression of cardiac arrhythmias [12,13].

In this paper we analyze two methods that have been suggested for employing time-delayed information to stabilize a periodic orbit. We investigate the control of a fixed point x^* of a one-dimensional discrete map

$$x_{n+1}=f(x_n;\kappa), \tag{1}$$

where $\kappa=\kappa_0+\epsilon_n$ is a parameter (nominal value κ_0) that can be adjusted by small amounts ϵ_n on each iterate of the map. The size of the adjustments is determined from a feedback algorithm that makes a comparison between the current state of the system x_n and its values on previous iterates; it does not make a comparison to the value of the fixed point x^* (the reference state used in the majority of feedback schemes). The simplest time-delay scheme for controlling the fixed point of the map is to take form [4–6]

$$\epsilon_n=\gamma(x_n-x_{n-1}), \tag{2}$$

where the gain γ is an appropriately chosen real number. This basic scheme has been called the discrete version of ''time delay autosynchronization'' (TDAS) [7,13].

We consider two schemes that have been suggested for generalizing TDAS by incorporating information from farther in the past than a single iterate. We report on detailed analyses of the parameter regimes in which these schemes are successful and on numerical measurements of the effect of noise on the controlled systems. The first scheme, termed ''extended TDAS'' (ETDAS) [7–11,14], uses an infinite series of past iterates with weights that decay exponentially with time in a form given by

$$\begin{aligned}\epsilon_n&=\gamma\sum_{k=0}^{\infty}R^k(x_{n-k}-x_{n-k-1})\\&=\gamma(x_{n-k}-x_{n-1})+R\epsilon_{n-1},\end{aligned} \tag{3}$$

where R is a real parameter with $|R|<1$. An important reason for investigating ETDAS feedback is that it can be generated experimentally using a recursive feedback loop with a single delay element and it has an all-optical implementation [7,11]. In some cases the physics of the system may not permit more complicated controller designs that might be suggested by control-theoretic analyses. A continuous version of ETDAS has been found, both analytically and experimentally, to be an improvement over TDAS [7–9,11,14], which corresponds to the special case $R=0$.

The second scheme, which we will call NTDAS, uses an average of N past iterates with equal weights in a form given by

$$\epsilon_n = \gamma\left(x_n - \frac{1}{N}\sum_{k=1}^{N} x_{n-k} \right). \tag{4}$$

NTDAS reduces to TDAS when N is set to 1. While this method is not easily implemented in high-speed systems, digital implementation for relatively slow systems is straightforward. NTDAS has been introduced into the physics literature by Flake *et al.* [15] and by Christini *et al.* [16,17]. We note that these two schemes differ from the recursive feedback algorithms investigated by Rollins and collaborators [18] in that their scheme makes a comparison to a known reference state (the value of the fixed point).

It is convenient to use the following quantities in discussing the controlled system. Let $\nu \equiv df(x^*)/dx$ be the Floquet multiplier associated with the fixed point of the uncontrolled map; i.e., $x_{n+1} - x^* = \nu(x_n - x^*)$ for $x_n - x^*$ sufficiently small. The uncontrolled fixed point is unstable if and only if $|\nu| > 1$. Let $\beta \equiv \gamma[df(x^*)/d\kappa]$ be the natural measure of the strength of the feedback gain. (Note that γ itself is not a useful measure since the effect of the feedback on the system depends on the degree to which changes in κ alter the trajectories.) The region in (ν,β) space where the fixed point is stable for various choices of R or N will be called the *domain of control*.

For both ETDAS and NTDAS, we wish to determine (1) the boundaries of the domain of control, (2) the nature of the bifurcation that occurs as β is varied so that the boundary of the domain of control is crossed, and (3) some measure of the robustness of the control that can be achieved by adjusting γ for a given choice of R or N and a given value of ν. Section II presents the linear stability analysis and determination of the Floquet multipliers for the case of ETDAS, addressing points (1) and (2). Section III presents a similar analysis for the case of NTDAS. Section IV addresses point (3): an analytical treatment of the effect of additive white noise is presented. Finally, Sec. V discusses some relevant points of comparison between the two methods.

II. LINEAR STABILITY ANALYSIS FOR ETDAS

The linear stability analysis for ETDAS can be carried out in a straightforward manner by linearizing Eqs. (1) and (3) about x^*, defining $z_n \equiv x_n - x^*$ and $e_n \equiv \epsilon_n/\gamma$, and rewriting the equations in the form

$$\begin{pmatrix} z_{n+1} \\ e_{n+1} \end{pmatrix} = \begin{pmatrix} \nu & \beta \\ \nu - 1 & \beta + R \end{pmatrix} \begin{pmatrix} z_n \\ e_n \end{pmatrix}. \tag{5}$$

The Floquet multipliers for the controlled system are the eigenvalues of the matrix in Eq. (5) given by

$$\mu_{\pm} = \frac{1}{2}[\nu + \beta + R \pm \sqrt{(\nu + \beta + R)^2 - 4(\nu R + \beta)}]. \tag{6}$$

Straightforward analysis (or application of the Shur-Cohn criteria) shows that ν and β must lie within the triangle defined by the lines

$$\nu = 1, \tag{7}$$

$$(1+R)\nu + 2\beta = -(1+R), \tag{8}$$

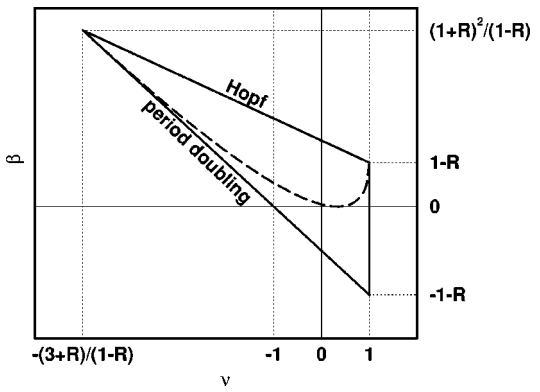

FIG. 1. Domain of control for ETDAS. For values of ν and β inside the triangular boundary the fixed point is stable. In the absence of control ($\beta = 0$), the fixed point would be stable only for $-1 < \nu < 1$. The dashed curve indicates the value of β for which the largest magnitude Floquet multiplier is made as small as possible for a given ν. The upper and lower boundaries of the domain of control are labeled by the type of bifurcation that occurs as they are crossed. The case $R = 1/3$ explicitly illustrated, but the axis labels are correct for any R.

$$R\nu + \beta = 1, \tag{9}$$

in order for both multipliers to have magnitude less than unity (i.e., the controller successfully stabilizes the fixed point). Figure 1 depicts this domain of control.

The following points are worth noting.

(1) ETDAS fails to control an unstable fixed point with positive multiplier, $\nu > 1$, for any choice of R and γ. (Choosing γ is equivalent to choosing β.)

(2) The most unstable fixed point that can be controlled for a given value of R has $|\nu| = (3+R)/(1-R)$, which can be made as large as desired by choosing R sufficiently close to 1.

(3) The optimal choice of β for robustness in the presence of noise differs markedly from the criterion that the Floquet multipliers of the controlled system be as small as possible. This point will be discussed further in Sec. IV.

The types of bifurcations encountered as β is adjusted for fixed values of ν and R are readily determined. Upon decreasing β so as to cross the lower boundary of the domain of control, μ_- passes through -1 and a period-doubling bifurcation occurs. Upon increasing β so as to cross the upper boundary of the domain of control, a supercritical Hopf bifurcation occurs. A branch of the curve $(\nu + \beta + R)^2 - 4(R\nu + \beta) = 0$ lies within the domain of control and is indicated by the dashed line in Fig. 1. For points above this line the eigenvalues form a complex conjugate pair. The rotation frequency ω_H of the limit cycle just beyond the Hopf boundary (the upper boundary of the domain of control) is given by the argument of μ_+ at the point where the boundary is crossed. Letting δ be defined by the relation $\nu = 1 - 4(\frac{1}{2} - \delta)/(1-R)$ so that the upper boundary is traversed from left to right as δ varies between $-1/2$ and $1/2$, we obtain

$$\omega_H = \tan^{-1}\left(\frac{\sqrt{1 - 4\delta^2}}{\delta} \right). \tag{10}$$

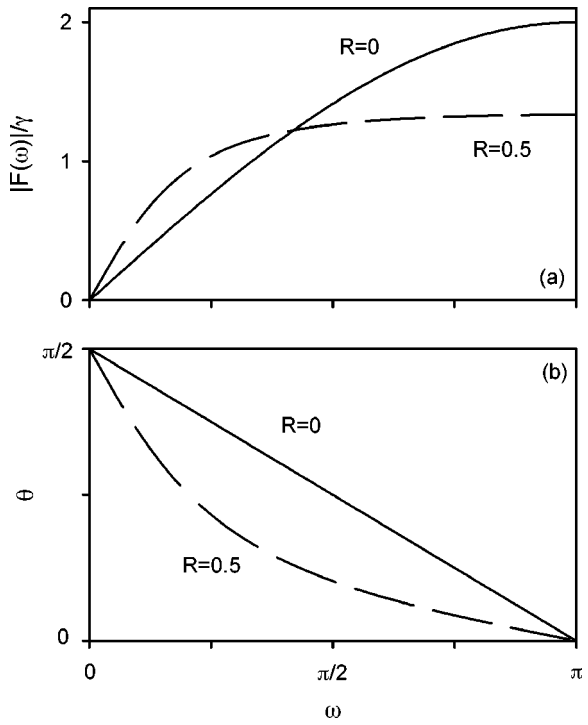

FIG. 2. Transfer function for the ETDAS controller for two different values of the parameter R. (a) Absolute value of the transmission through the filter as a function of frequency. (b) Phase characteristics of the filter.

As may have been expected, ω_H approaches π at the leftmost point, which is where the Hopf line and period-doubling line meet, and approaches 0 at the rightmost point, which is where the Hopf line meets $\nu=1$, corresponding to pure expansion with no oscillation.

In designing devices for generating feedback signals, it is often useful to consider the behavior of the controller in the frequency domain in addition to the time-domain stability analysis given above. For the case of discrete maps, we take each iterate to correspond to a unit interval of time. Note that the ETDAS feedback signal linearly relates the input signal x with the output signal ϵ; hence $\epsilon(\omega)=F(\omega)x(\omega)$, where $x(\omega)$ and $\epsilon(\omega)$ are the Fourier amplitudes of the input and output signals, respectively, and

$$F(\omega)=\gamma\frac{1-e^{-i\omega}}{1-Re^{-i\omega}} \tag{11}$$

is the transfer function for ETDAS feedback. The transfer function ''filters'' the observed state of the dynamical systems, characterized by $x(\omega)$, to produce the necessary feedback signal $\epsilon(\omega)$. Due to the discrete nature of the system, it is sufficient to consider the transfer function $F(\omega)$ of the controller in the interval $0\leqslant\omega\leqslant\pi$.

Figure 2 shows $|F(\omega)|$ and $\theta=\tan^{-1}[\mathrm{Im}\,F(\omega)/\mathrm{Re}\,F(\omega)]$ for $R=0$ (TDAS) and $R=0.5$ (ETDAS). It is seen that there is a notch dropping to zero at $\omega=0$, and the notch becomes narrower and the phase θ is closer to zero over a larger frequency extent for larger R. The existence of the notch in the transfer function can be understood easily by considering that ϵ_n, and hence $\epsilon(\omega)$, must vanish when the fixed point is stabilized. Recall that the spectrum of the system $x(\omega)$ when it is on the fixed point consists of a δ function at $\omega=0$; therefore, the filter must remove this frequency (via the notch) so that $\epsilon(\omega)=0$. The ETDAS feedback is more effective in stabilizing the fixed point for larger R partly because it is more sensitive to frequencies that could potentially destabilize the fixed point. The narrow notch implies that more feedback is generated for signals with frequency components slightly different than the desired one. In addition, $|F(\omega)|$ remains near one and θ is closer to zero for larger R, and so the system is less likely to be destabilized by a large, out-of-phase feedback response at these intermediate frequencies.

III. LINEAR STABILITY ANALYSIS FOR NTDAS

The boundaries of the domain of control for a system controlled by NTDAS can be obtained in closed form as parametric equations. The linearized equations in the vicinity of the fixed point can be written in matrix form as

$$\begin{pmatrix} z_{n+1} \\ z_n \\ z_{n-1} \\ \vdots \\ z_{n-N+1} \end{pmatrix} = \begin{pmatrix} \nu+\beta & -b & -b & \cdots & -b \\ 1 & 0 & 0 & \cdots & 0 \\ 0 & 1 & 0 & & \\ \vdots & & \ddots & \ddots & \\ 0 & \cdots & 0 & 1 & 0 \end{pmatrix} \times \begin{pmatrix} z_n \\ z_{n-1} \\ z_{n-2} \\ \vdots \\ z_{n-N} \end{pmatrix}, \tag{12}$$

where $b\equiv\beta/N$. It is immediately clear that the determinant of the matrix is $\pm b$, which means that the system must be unstable for $b>1$ or $\beta>N$. This turns out to be important only for the case $N=1$, which is the case of TDAS and is easily analyzed. (It is the case $R=0$ in Fig. 1, for which the upper boundary becomes a horizontal line at $\beta=1$.)

For $N>1$, the characteristic equation for the matrix is

$$\mu^N(\nu+\beta-\mu)-b\sum_{k=0}^{N-1}\mu^k=0. \tag{13}$$

On the boundaries of the domain of control we must have a solution with $|\mu|=1$, and conversely, any values of ν and β for which a solution with $|\mu|=1$ exists must be either on the boundary or outside the domain of control. (It can be outside if for those same values there exists another solution with $|\mu|>1$.)

We first note that $\mu=1$ is a solution of Eq. (13) if and only if $\nu=1$, and it is easily verified that there is always a solution with $\mu>1$ for any $\nu>1$. Next note that $\mu=-1$ is a solution if and only if

$$\beta=\frac{-N(1+\nu)}{N+\mathrm{mod}_2 N}. \tag{14}$$

This line constitutes a boundary of the domain of control corresponding to a period-doubling bifurcation. (See Fig. 3.)

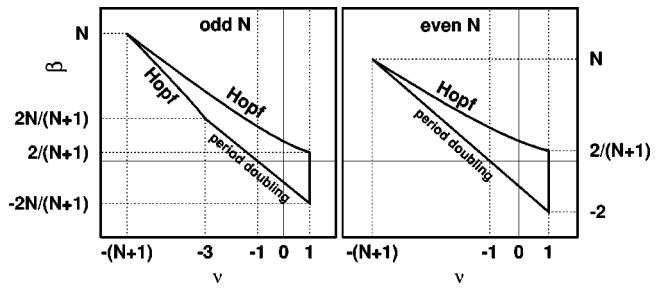

FIG. 3. Domain of control for NTDAS. For values of ν and β inside the heavy boundary the fixed point is stable. In the absence of control ($\beta=0$), the fixed point would be stable only for $-1<\nu<1$. The case $N=5$ and $N=4$ are shown as representatives of odd and even N. The axis labels are correct for any N. The upper and lower boundaries of the domain of control are labeled by the type of bifurcation that occurs as they are crossed.

For any ν other than 1, we can multiply by $1-\mu$ and rearrange terms to obtain

$$\mu^N[\mu^2-(\nu+\beta+1)\mu+\nu+\beta+b]=b. \tag{15}$$

Letting $\mu=\exp(i\phi)$, the real and imaginary parts of this equation give two relations involving ϕ, ν, and β that must be satisfied on the boundary of the domain of control. These can be solved for ν and β in terms of ϕ, yielding

$$\nu=\frac{-(1+2N)s_1+(1+N)s_2+s_{N+1}-s_{N+2}}{s_1+s_N-s_{N+1}}, \tag{16}$$

$$\beta=\frac{2Ns_1-Ns_2}{s_1+s_N-s_{N+1}}, \tag{17}$$

where $s_n\equiv\sin(n\phi)$.

To map out the remaining portions of the boundary, the appropriate values of ϕ must be determined. This can be accomplished by noting that at the special point $(\nu,\beta)=(-N-1,N)$, Eq. (15) reduces to $\mu^{N+2}=1$, so that all of the Floquet multipliers have unit magnitude. As ϕ is increased from zero, this point is first reached at $\phi=2\pi/(N+2)$, and so it is values of ϕ in the interval $[0,2\pi/(N+2)]$ that produce the upper boundary in Fig. 3. This boundary corresponds to a Hopf bifurcation with rotation frequency $\omega_H=\phi$. For even N, the lower (period-doubling) boundary already determined passes through the special point and the entire domain has now been determined. For odd N, there is an additional section of the boundary that is obtained by allowing ϕ to decrease from its period-doubling value of π until it first reaches one of the $(N+2)$th roots of unity; i.e., $\phi\in[\pi(N+1)/(N+2),\pi]$. This section of the boundary also corresponds to a Hopf bifurcation. Taking the limit of Eq. (16) as ϕ approaches π from below, one finds that this curve intersects the period-doubling boundary at $\nu=3$. Figure 3 shows the domains of control for the cases of even and odd N.

Parallel to the discussion in the previous section, we explore the frequency-domain response of NTDAS feedback. The transfer function is found by Fourier transforming Eq. (4) and is given by

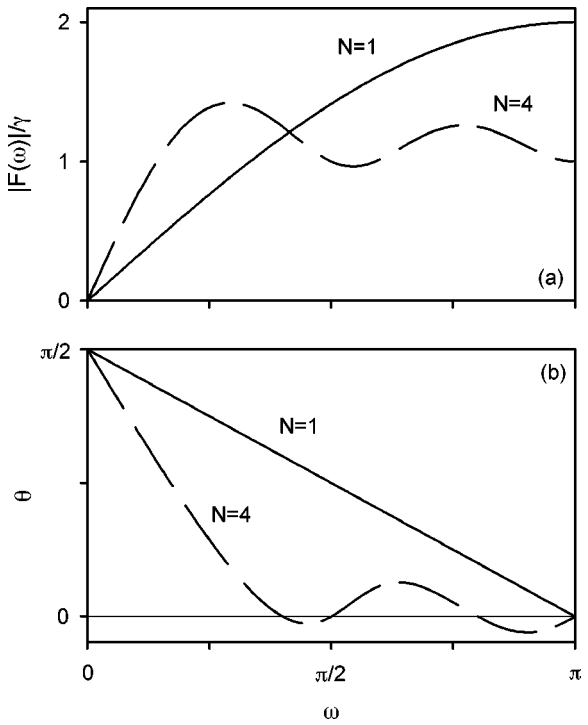

FIG. 4. Transfer function for the NTDAS controller for two different values of the parameter N. (a) Absolute value of the transmission through the filter as a function of frequency. (b) Phase characteristics of the filter.

$$F(\omega)=\left[1-\frac{e^{-i\omega}\ (1-e^{-iN\omega})}{N(1-e^{-i\omega})}\right]. \tag{18}$$

Figure 4 shows $|F(\omega)|$ and $\theta=\tan^{-1}[\mathrm{Im}\ F(\omega)/\mathrm{Re}\ F(\omega)]$ for $N=0$ (TDAS) and $N=4$ (NTDAS). As for ETDAS feedback discussed in the previous section, the notch at $\omega=0$ becomes narrower and the phase θ is closer to zero over a larger frequency extent for larger N, although the curves oscillate about their nominal values. Note that θ approaches zero at a lower frequency in comparison to ETDAS feedback (albeit with oscillations), suggesting that NTDAS feedback may be less sensitive to perturbations over a broader frequency range in comparison to ETDAS. See the discussion on noise sensitivity in the following section.

IV. ROBUSTNESS OF ETDAS AND NTDAS IN THE PRESENCE OF NOISE

Determing the noise amplitude at which linear control fails requires a comparison of the size of the deviations from the linearized equations induced by the noise with the original noise level itself [19]. Control will fail when the nonlinear deviations, or ''deviational noise,'' become comparable in magnitude to the original additive noise. To estimate the size of the deviational noise, one may first determine the extent to which the additive noise is amplified in the purely linear system, then consider the strength of the nonlinearity. Let σ be the additive noise strength (the rms magnitude of the noise added to x_n on each iteration); assume that the dominant nonlinearity in the vicinity of the fixed point is cz^λ, and let the noise amplitude that would be generated by the purely linear system with control applied be $\alpha\sigma$, where

the amplification factor α is a function of the system parameters and control parameters. A rough criterion for the maximum noise that can be tolerated is

$$c(\alpha\sigma_{\max})^{\lambda}=\sigma_{\max}, \tag{19}$$

which gives accurate estimates for generic nonlinearities and noise characteristics. (For engineering applications in which it is imperative that one obtain conservative bounds, standard control-theoretic methods of analysis are available [20].)

In this paper, we do not specify the nature of the nonlinearity in the system. Nevertheless, by computing α for different control parameters we can determine which choice will give the optimal noise tolerance, regardless of the precise values of c and λ. Note that for any linearized system σ can be scaled arbitrarily, and so there is no threshold for loss of control in the purely linear system.

To determine the amount of amplification of the noise in the time-delay controlled systems of interest here, we consider first an arbitrary stable linear system to which noise is added only to the first component in a form given by

$$\mathbf{z}_{n+1}=\mathbf{M}\cdot\mathbf{z}_n+\boldsymbol{\eta}_n, \tag{20}$$

where $\mathbf{M}$ is a real $L\times L$ matrix and $\boldsymbol{\eta}_n=[\eta_n,0,0,\ldots]^T$, with η_n being unbiased and δ correlated so that

$$\langle\eta_n\rangle=0 \quad \forall n, \tag{21}$$

$$\langle\eta_n\eta_m\rangle=\sigma^2\delta_{nm}. \tag{22}$$

Let $\mathbf{E}$ be the matrix of (right) eigenvectors of $\mathbf{M}$, with element E_{ij} equal to the ith component of the jth eigenvector, let $\mathbf{V}$ be the inverse of $\mathbf{E}$, and let $\mu_{(j)}$ be the eigenvalue associated with the jth eigenvector.

Taking $\mathbf{z}_0$ as a given initial condition, we have

$$\mathbf{z}_{n+1}=\mathbf{M}^n\cdot\mathbf{z}_0+\sum_{m=0}^{n}\mathbf{M}^{n-m}\cdot\boldsymbol{\eta}_m. \tag{23}$$

For $n\to\infty$, the first term vanishes since the controlled system is stable in the absence of noise. Using Eqs. (21) and (22) it is found that the average value of $|z_1|^2$ after many iterations approaches

$$\langle|z_1|^2\rangle=\sum_{i,j}\frac{V_{i1}^*V_{j1}E_{1i}^*E_{1j}}{1-\mu_{(i)}^*\mu_{(j)}}. \tag{24}$$

The amplification factor α is defined as $\langle|z_1|^2\rangle^{1/2}/\sigma$.

For either ETDAS or NTDAS, α can be determined for any given choice of ν, β, and R or N from the matrices given above. The results are illustrated in Fig. 5. In panels (a) and (b), each curve shows α as a function of β for a fixed value of ν, with the values of β spanning the width of the domain of control. In panel (a), which corresponds to ETDAS with $R=0.5$, the large dot on each curve indicates the value of β corresponding to the smallest maximum multiplier, and it is clear that this point does not correspond to the lowest noise amplification. The lowest noise amplification is achieved closer to the center of the domain of control, as might have been expected intuitively. Panel (b) shows results for NTDAS with $N=4$. This value of N was chosen for comparison because it corresponds to the number of iterates for which the weights used in ETDAS with $R=0$ become small, with the criterion for smallness being arbitrarily chosen at 5% of the weight of the first iterate.

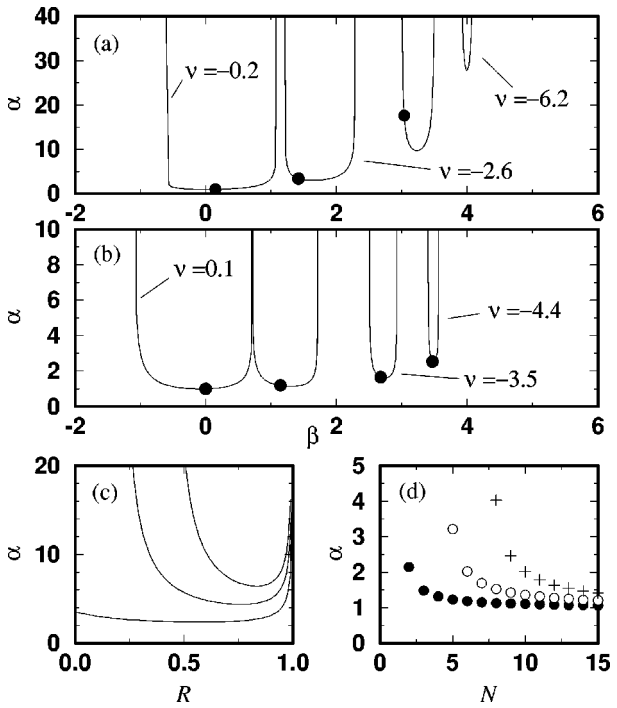

FIG. 5. The amplification of noise by ETDAS and NTDAS controllers. (a) ETDAS control with $R=0.5$. Each curve corresponds to a fixed value of ν and spans the values of β within the domain of control for that ν. From left to right, the values of ν are -0.2, -2.6, -5.0, and -6.2. The heavy dot on each curve indicates the value of β for which the eigenvalues have the lowest magnitude, which are clearly seen to differ from the values that give the lowest noise amplification. The heavy dot on the right most curve lies on the left branch at $\alpha\approx 84$. (b) NTDAS control with $N=4$. Values of ν used in this case are 0.1, -1.7, -3.5, and -4.4. No control is possible in this case for $\nu<-5$. Note the different vertical scale from part (a). (c) Variation of α with R for fixed ν. The lower, middle, and upper curves correspond to $\nu=-2$, -4, and -6, resepctively. For each point on each curve β is chosen near the center of the domain of control, as described in the text. (d) Variation of α with N for fixed ν. The lower, middle, and upper curves correspond to $\nu=-2.5$, -5.5, and -8.5, resepctively. For each point on each curve β is chosen near the center of the domain of control, as described in the text.

Figure 5(c) shows how α varies at fixed ν for different values of R in ETDAS, indicating a clear minimum in noise amplification for R in the range 0.6–0.8. For these plots β is chosen at the midpoint of the domain of control for the appropriate values of ν and R; i.e., $\beta=(1-R-\nu-3R\nu)/4$. Each curve corresponds to a different value of ν. Figure 5(d) shows how α varies at a fixed ν for different values of N in

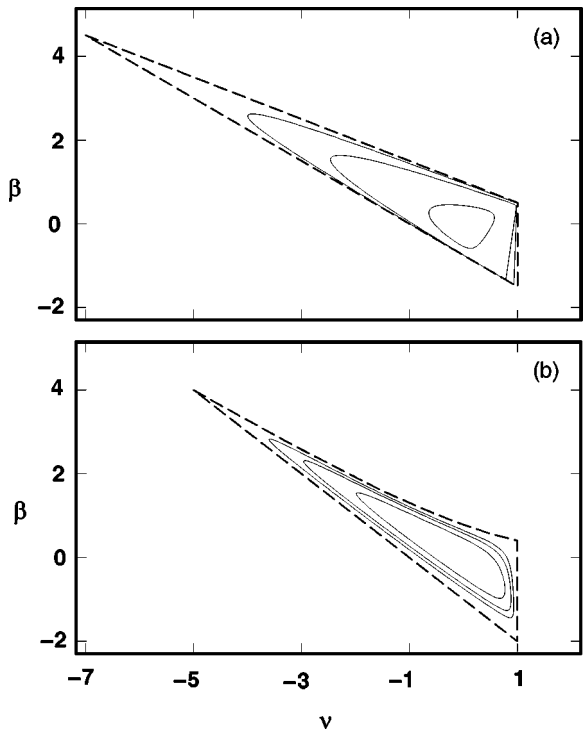

FIG. 6. Contour plots of noise sensitivity for (a) ETDAS control with $R=0.5$ and (b) NTDAS control for $N=4$. The dashed lines indicate the boundary of the domain of control. In (a), the contours correspond to $\alpha=\sqrt{2}$, 8, and 32, and in (b) they correspond to $\sqrt{2}$, 2, and $\sqrt{2}$, where the lowest area contour is for the smallest value of α.

NTDAS, indicating that larger values of N provide better performance. For these plots β is taken to be $-\nu N/(N+1)$, which is near the midpoint of the domain of control.

The noise sensitivity of the two control schemes for fixed R and N can be visualized quickly by a contour plot of α in the ν-β plane, as shown in Fig. 6. Consistent with Fig. 5, it is seen that the region of low noise sensitivity is confined to the center of the domain of control and to small values of $|\nu|$. In addition, it is seen that the region of low noise sensitivity for NTDAS extends over a larger range than ETDAS, suggesting that is may be the control scheme of choice in high-noise situations and when it is feasible to generate the NTDAS feedback signal.

To confirm the validity of the criterion of Eq. (19), we have numerically iterated an ETDAS-controlled map of the form $f(x)=\nu x_n+cx_n^{\lambda}$, taking c to be 10 and λ to be 2 or 3. The criterion indicates that the effect of noise will be most dramatic where α is large. This occurs for all values of ν and R if γ is chosen so as to place the system very near the boundary of the domain of control. More importantly, however, one is forced to a region of large α if control of a highly unstable fixed point, say, $\nu=-50$, is desired. Choosing $R=0.95$ and then setting γ so as to minimize α, we find $\alpha\approx 77$. For $\lambda=2$ (or 3) the noise tolerance criterion implies that control should fail for $\sigma>2\times10^{-5}$ (or 5×10^{-4}). We have iterated the equations

$$z_{n+1}=\nu z_n+cx_n^{\lambda}+\epsilon_n+\eta_n, \tag{25}$$

$$\epsilon_n=\gamma(z_n-z_{n-1})+R\epsilon_{n-1}, \tag{26}$$

with η_n uniformly distributed in the interval $(-\sqrt{3}\sigma,\sqrt{3}\sigma)$ for increasing σ. We find that control is lost at $\sigma=7\times10^{-5}$ for $\lambda=2$ and $\sigma=6\times10^{-4}$ for $\lambda=3$, both of which are in reasonable agreement with the estimates. The determination that control is lost is made easily in these systems by monitoring the value of $|x_n|$. When control is successful, the maximum value of $|x_n|$ over many (10 000) iterations lies within about 10% of $\alpha\sigma$. When control is lost, x_n diverges rapidly. The smallest value of σ for which control is lost depends only weakly on the number of iterates monitored. The quoted results changed by less than 1% when 10 times as many iterates were monitored.

V. CONCLUSIONS

We have investigated two feedback schemes for stabilizing the dynamics of discrete maps about unstable fixed points. The techniques do not require a comparison to a reference state; rather, they make a comparison of the current state of the system with past iterates of the map. In addition, the techniques we have studied permit generalization to a continuous mode of operation, which might be necessary in fast systems. (References [7,8,11,14] discuss the continuous version of ETDAS.)

Our analysis reveals that the domains of control for ETDAS (characterized by feedback parameter R) and NTDAS (characterized by feedback N) are roughly comparable when $R^N\sim0.05$. We also find that NTDAS is somewhat more tolerant to uniform noise over the entire domain of control in comparison to ETDAS, which is counterbalanced by the fact that NTDAS is somewhat more difficult in analog systems. It should be noted that a third technique has been suggested, in which the feedback signal is switched off for every other iterate of the map [5]. This approach has certain advantages, especially in that it permits stabilization of maps with postive ν, though it is by nature not suitable for continuous operation. It has not been treated in detail here only because a parallel treatment would require some (possibly subtle) extensions of our methods of analysis. Our purpose here is to examine two schemes that have received some attention recently, not to argue for their optimality over all other conceivable approaches.

We conjecture that both ETDAS and NTDAS are suitable for tracking trajectories in the presence of slow parameter drift as long as β can be continually adjusted so that the system remains within the domain of control. An intriguing possibility is that the noise level itself could be used as a measure of parameter drift and used to make slow adjustments to β. Depending on the parameter regime of interest, this might be *easier* to do with ETDAS, since the noise sensitivity varies more rapidly as a function β, whereas for NTDAS the noise level increases only very slightly until one gets very close to the stability boundary.

Finally, our analysis of noise amplification serves as an example which should be of interest to physicists designing feedback-control devices. As is well documented in the control theory literature, the fact that a system possesses only stable Floquet multipliers gives no guarantee of robust operation. Trefethen has emphasized that the interaction of

nonlinearities with transient growth that may occur in the linearized system can result in extreme sensitivity to noise [21]. We have shown a simple way to obtain a measure of the level of noise that can be tolerated by a given controller and presented an example in which control is lost at noise levels for which the nonlinear terms associated with bare noise appear at first glance to be negligibly small.

ACKNOWLEDGMENTS

This work was supported by funds from the Whitaker Foundation (D.J.G.), the U.S. ARO through Grant No. DAAH04-94-G-0174 (D.G.J.), and the NSF through Grant Nos. PHY-9357234 (D.J.G.) and Nos. DMR-9412416 (J.E.S.S.).

[1] E. Ott and M. Spano, Phys. Today **48** (5), 34 (1995).
[2] E. Ott, C. Grebogi, and J. A. Yorke, Phys. Rev. Lett. **64**, 1196 (1990).
[3] F. J. Romeiras, C. Grebogi, E. Ott, and W. P. Dayawansa, Physica D **58**, 165 (1992).
[4] K. Pyragas, Phys. Lett. A **170**, 421 (1992).
[5] S. Bielawski, D. Derozier, and P. Glorieux, Phys. Rev. E **49**, R971 (1994).
[6] D. J. Gauthier, D. W. Sukow, H. M. Concannon, and J. E. S. Socolar, Phys. Rev. E **50**, 2343 (1994).
[7] J. E. S. Socolar, D. W. Sukow, and D. J. Gauthier, Phys. Rev. E **50**, 3245 (1994).
[8] M. E. Bleich and J. E. S. Socolar, Phys. Lett. A **210**, 87 (1996).
[9] M. E. Bleich and J. E. S. Socolar, Phys. Rev. E **54**, R17 (1996).
[10] M. E. Bleich, D. Hochheiser, J. V. Moloney, and J. E. S. Socolar, Phys. Rev. E **55**, 2119 (1997).
[11] D. W. Sukow, M. E. Bleich, D. J. Gauthier, and J. E. S. Socolar, Chaos **7**, 560 (1997).
[12] K. Hall, D. J. Christini, M. Tremblay, J. J. Collins, L. Glass, and J. Billette, Phys. Rev. Lett. **78**, 4518 (1997).
[13] D. J. Gauthier and J. E. S. Socolar, Phys. Rev. Lett. **79**, 4938 (1997).
[14] K. Pyragas, Phys. Lett. A **206**, 323 (1995).
[15] G. W. Flake, G.-Z. Sun, Y.-C. Lee, and H.-H. Chen, in *Advances in Neural Information Processing*, edited by J. D. Cowan, G. Tesauro, and J. Alspector (Morgan Publishers, San Mateo, CA, 1994), p. 647.
[16] D. J. Christini, V. In, M. L. Spano, W. L. Ditto, and J. J. Collins, Phys. Rev. E **56**, R3749 (1997).
[17] D. J. Christini and J. J. Collins, IEEE Trans. Circuits Syst. **44**, 1027 (1997).
[18] R. W. Rollins, P. Parmananda, and P. Sherard, Phys. Rev. E **47**, R3003 (1993).
[19] D. A. Egolf and J. E. S. Socolar, Phys. Rev. E **57**, 5271 (1998).
[20] See, for example, J. C. Doyle, B. A. Francis, and A. R. Tannenbaum, *Feedback Control Theory* (Macmillan, New York, 1992).
[21] L. N. Trefethen, A. E. Trefethen, S. C. Reddy, and T. A. Driscoll, Science **261**, 578 (1993).